Supporting Information For:

Design of a Bioactive Small Molecule that Targets the Myotonic Dystrophy Type 1 RNA *Via* an RNA Motif-Ligand Database & Chemical Similarity Searching

Raman Parkesh[†a], Jessica L. Childs-Disney[†a], Masayuki Nakamori[‡], Amit Kumar[†], Eric Wang[§], Thomas Wang[§], Jason Hoskins[‡], Tuan Tran[†], David Housman[§], Charles A. Thornton[‡], and Matthew D. Disney[†]*

[†]Department of Chemistry, Scripps Florida, 130 Scripps Way, Jupiter, FL 33458
[‡]Department of Neurology, University of Rochester, Rochester, NY 14642
[§]Department of Biology, Massachusetts Institute of Technology, 31 Ames Street, 68-132, Cambridge, MA 02139
Disney@scripps.edu

[a]these authors contributed equally to this work

*author to whom correspondence should be addressed

Contents

1. Full Citation for Reference 14.

Brook, J. D., McCurrach, M. E., Harley, H. G., Buckler, A. J., Church, D., Aburatani, H., Hunter, K., Stanton, V. P., Thirion, J. P., Hudson, T., Sohn, R., Zemelman, B., Snell, R. G., Rundle, S. A., Crow, S., Davies, J., Shelbourne, P., Buxton, J., Jones, C., Juvonen, V., Johnson, K., Harper, P. S., Shaw, D. J., and Housman, D. E. (1992) Molecular basis of myotonic dystrophy: expansion of a trinucleotide (CTG) repeat at the 3' end of a transcript encoding a protein kinase family member, *Cell 68*, 799-808.

2. General Methods

Mass Spectroscopy and HPLC Purification

Mass spectra were collected on a Varian 500 MS spectrometer equipped with Varian Prostar Autosampler 410 and/or on ABI 4800 MALDI-TOF spectrometer.

HPLC purifications were completed on a Waters 1525 Binary HPLC Pump equipped with a Waters 2487 Dual Absorbance Detector system. Compounds were purified using a gradient of 5mL/min, and a linear gradient of 0% to 100% B in A over 55, or 50, or 46 min. (A: water + 0.1% trifluoroacetic acid (TFA) (v/v); B: MeOH + 0.1%TFA (v/v).)

The purities of compounds were determined by analytical HPLC using a Waters 1525 Binary HPLC Pump equipped with Waters 2487 Dual λ Absorbance Detector system and the following conditions: a Waters Symmetry® C8 5µm 4.6×150 mm column, room temperature, a flow rate of 2.4 mL/min, and a linear gradient of 0% to 100% B in A over 45 min. A is 0.1% TFA in water while B is 0.1% TFA in methanol.

3. Characterization of Compounds from Small Molecule Libraries

Table S-1: HPLC retention times and masses of compounds showing 3D similarity to pentamidine.

Compound ID	Chemical Formula	HPLC Retention Time (min)	Mass (MH^+, Calculated)	Mass (MH^+, Found)
P1	$C_{22}H_{21}N_7O_2$	29	416.1	416.4
P2	$C_{22}H_{20}N_6O_2$	30	401.1	401.3
P3	$C_{22}H_{22}N_8O_2$	27	431.1	431.3
P4	$C_{24}H_{28}N_{10}O_2$	23	489.2	489.3
P5	$C_{15}H_{17}N_3O_2$	18	272.1	272.3
P6	$C_{22}H_{22}N_8O_2$	29	431.1	431.3
P7	$C_{14}H_{12}Cl_2N_2O$	32	295.0	295.1
P8	$C_{24}H_{26}N_8$	19	427.2	427.3

Table S-2: HPLC retention times and masses of compounds showing 3D similarity to Hoechst.

Compound ID	Molecular Formula	HPLC Retention Time (min)	Mass (Calculated)	Mass (Found)
H1	$C_{20}H_{20}N_6$	27	417.1 ($M+H^+$)	417.2 ($M+H^+$)
H2	$C_{21}H_{22}N_{10}$	24	415.2 ($M+H^+$)	415.3 ($M+H^+$)
H3	$C_{28}H_{37}NO_4$	28	453.2 ($M+H^+$)	453.3 ($M+H^+$)
H4	$C_{22}H_{20}N_6O_2$	28	401.1 ($M+H^+$)	401.3 ($M+H^+$)
H5	$C_{15}H_{12}F_3N_3$	27	292.1 ($M+H^+$)	292.2 ($M+H^+$)
H6	$C_{21}H_{24}N_4O$	25	377.2 ($M+H^+$)	377.3 ($M+H^+$)
H7	$C_{26}H_{24}N_6O_2$	25	453.2 ($M+2H^+$)	453.3 ($M+2H^+$)
H8	$C_{15}H_{14}N_2O_2$	31	255.1 ($M+H^+$)	255.2 ($M+H^+$)
H9	$C_{21}H_{23}N_7O_2$	21	406.1 ($M+H^+$)	406.3 ($M+H^+$)

4. Synthesis of H1 (5057-2468)

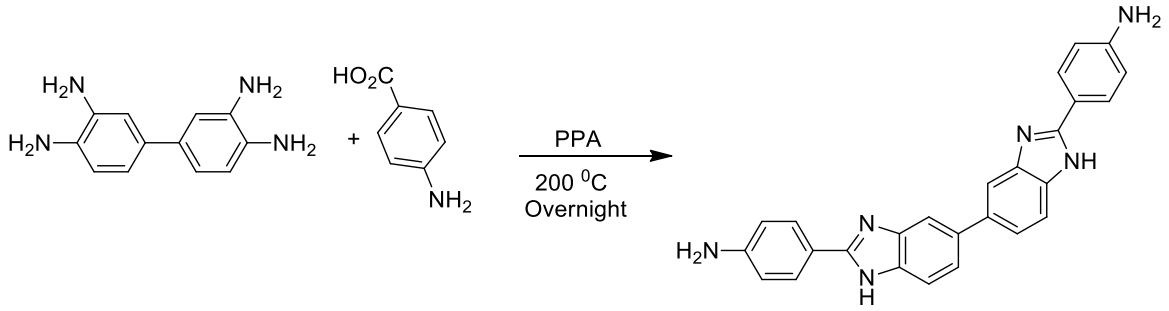

Scheme S-1: Reaction scheme for the synthesis of H1 (5057-2468).

Synthesis of 4,4'-(1H,1'H-[5,5'-bibenzo[d]imidazole]-2,2'-diyl)dianiline (H1): H1 was synthesized based on a previously reported patent.(*1*) Briefly, biphenyl-3,3',4,4'-tetramine (100 mg, 0.46 mmol) and 4-aminobenzoic acid (128 mg,0.92 mmol) were dissolved in 20 mL of polyphosphoric acid (PPA) and heated at 200 ^{o}C with stirring overnight. The mixture was cooled to room temperature and poured into water. The resulting mixture was stirred and a green solid was obtained. The solid was filtered and washed with saturated aqueous K_2CO_3 solution (100 mL). The solid was dissolved in methanol and treated with activated carbon. After filtering the activated carbon, the solution was evaporated to afford yellow solid, which was purified by flash column chromatography using EtOAc : MeOH (90:10, v/v) (80 mg, 45% yield). ESI-MS: Calculated ($M+H^+$): 417; Observed ($M+H^+$): 417. ^{1}H-NMR (DMSO, 400MHz): 5.62 (bs, 4H), 6.69 (d, 4H, *J*=8.8), (d, 4H, *J*=8.8), 7.41-7.75(m, 6H), 7.89 (d, 4H, *J*=8.8). ^{13}C-NMR(DMSO, 100MHz): 153.0, 150.5, 137.3, 137.0, 134.8, 130.9, 127.2, 122.3, 120.2, 117.4, 112.9.

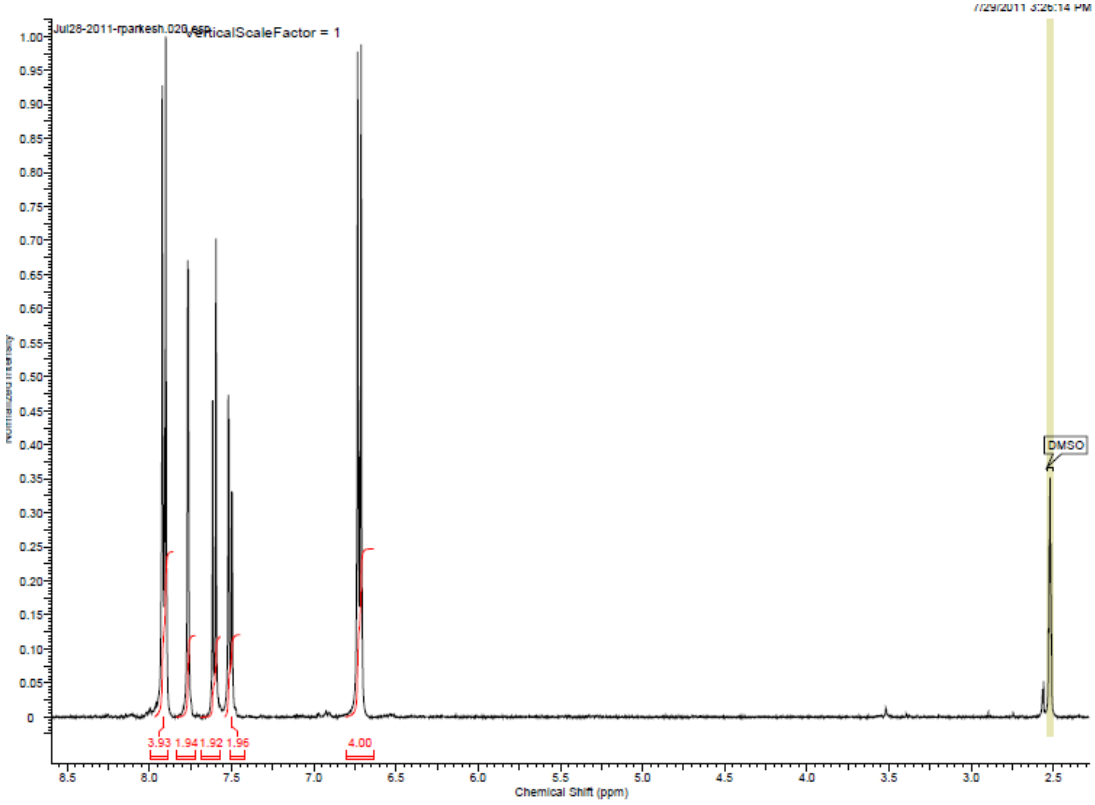

Figure S-1: H-1 NMR spectrum of H1 (5057-2468).

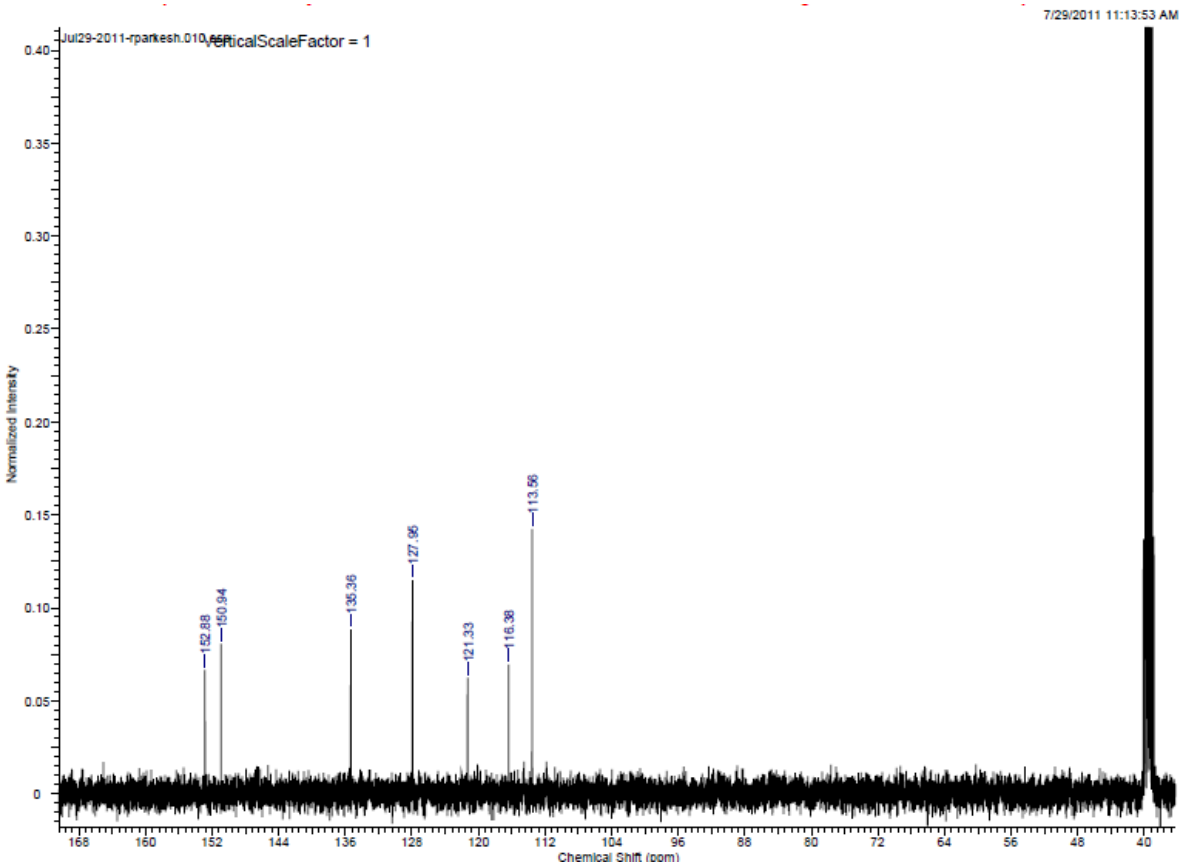

Figure S-2: Carbon-13 NMR spectrum for H1 (5057-2468).

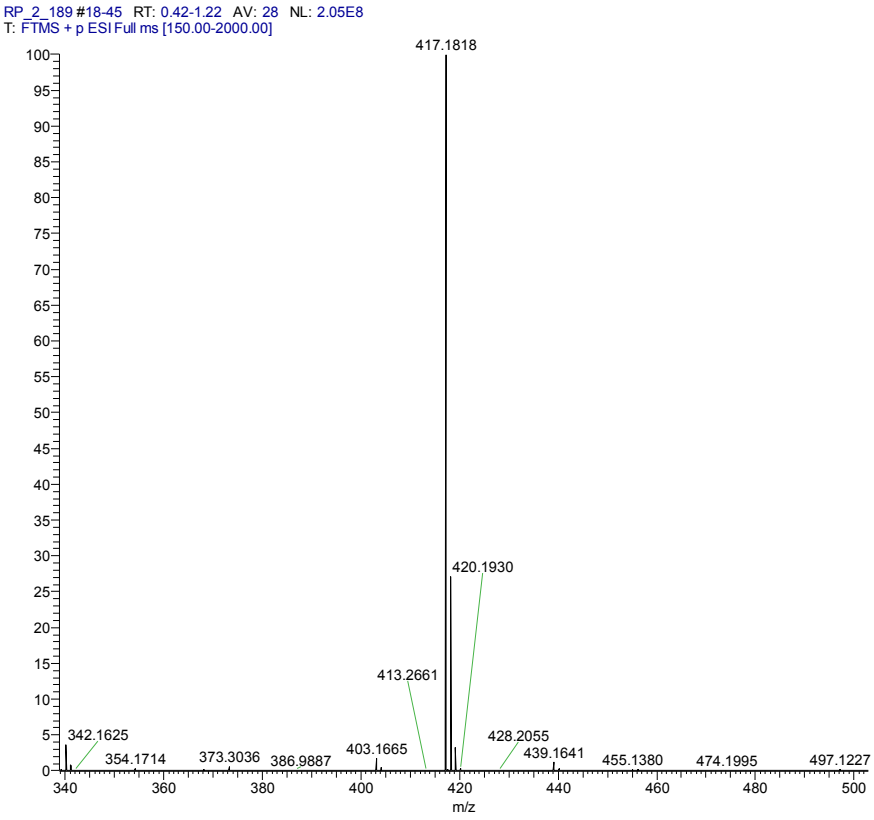

Figure S-3: High resolution mass spectrum for H1 (5057-2468).

5. Analytical HPLC Chromatograms of Compounds from Small Molecule Libraries

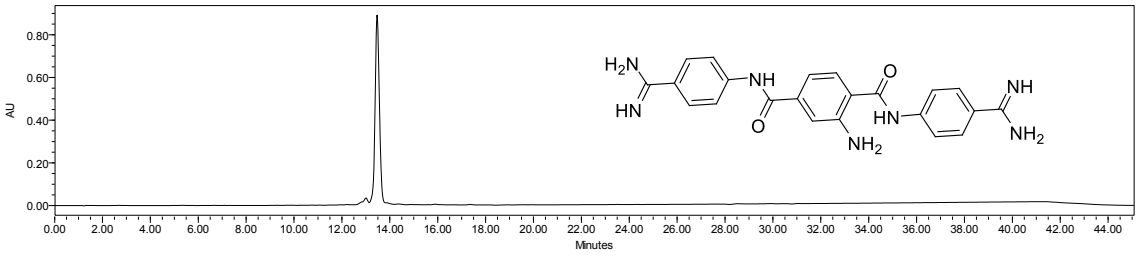

Figure S-4: Analytical HPLC trace of P1.

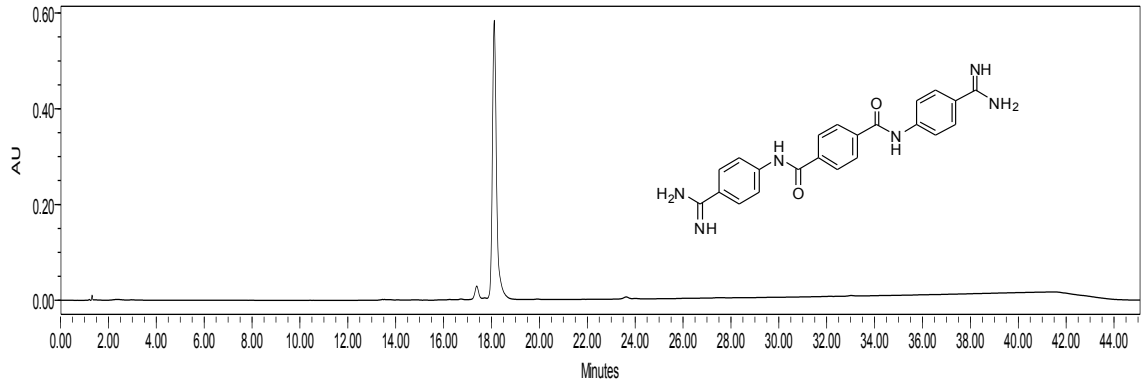

Figure S-5: Analytical HPLC trace of P2.

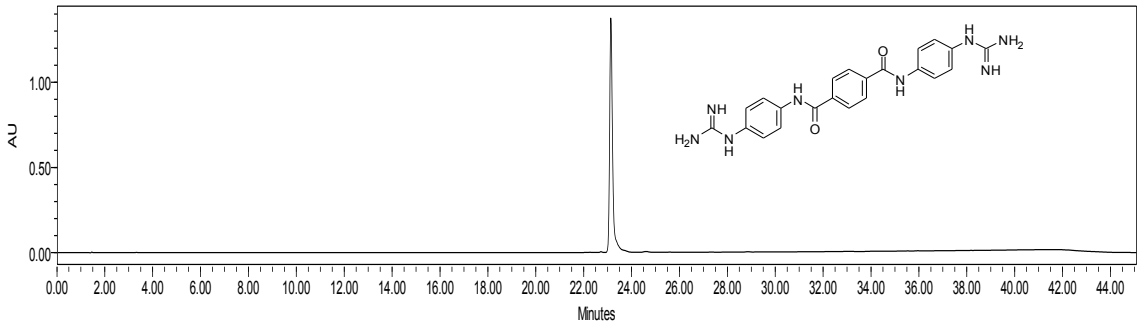

Figure S-6: Analytical HPLC trace of P3.

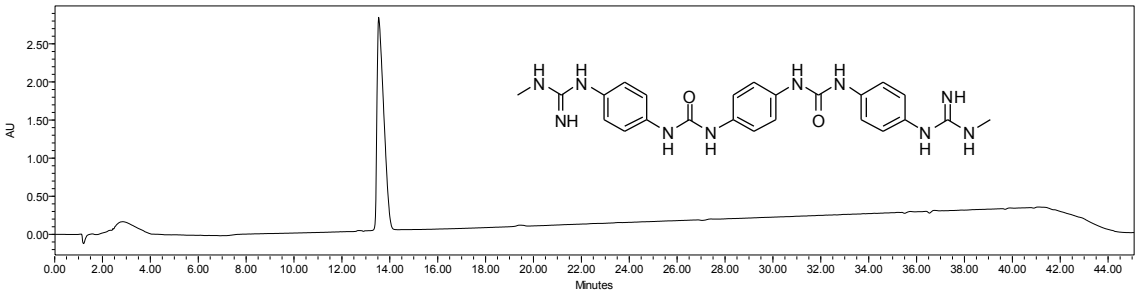

Figure S-7: Analytical HPLC trace of P4.

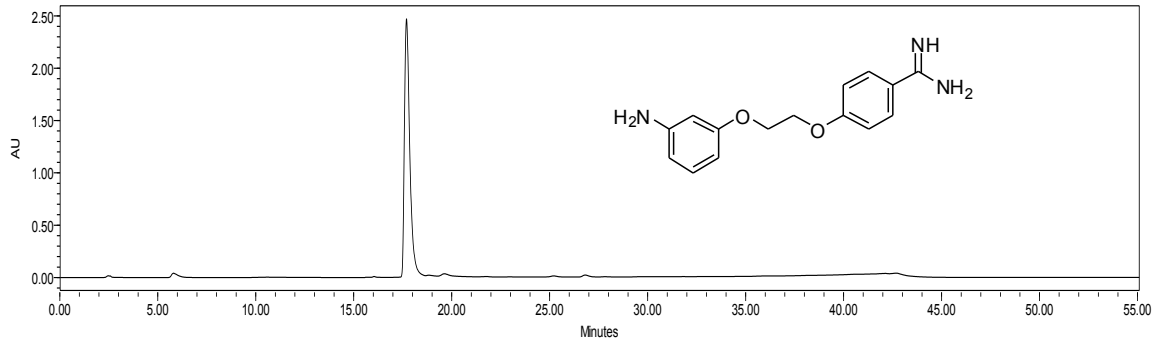

Figure S-8: Analytical HPLC trace of P5.

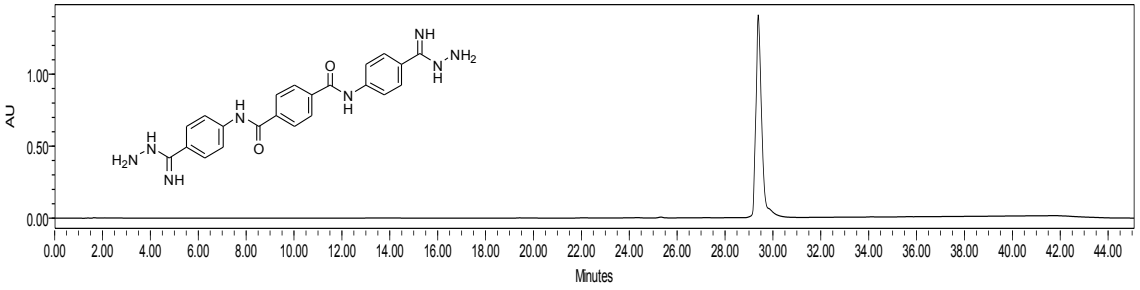

Figure S-9: Analytical HPLC trace of P6.

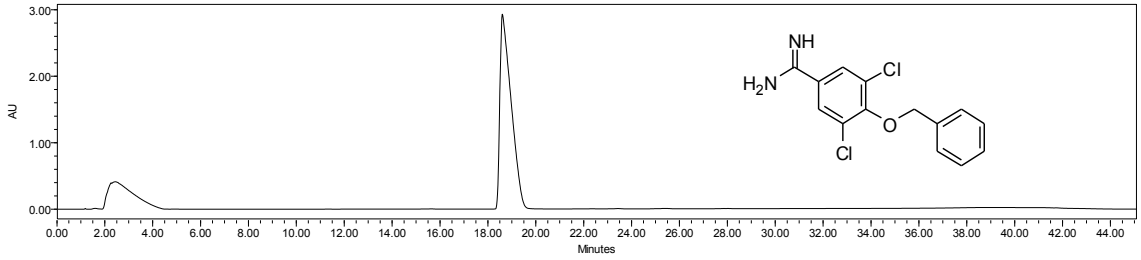

Figure S-10: Analytical HPLC trace of P7.

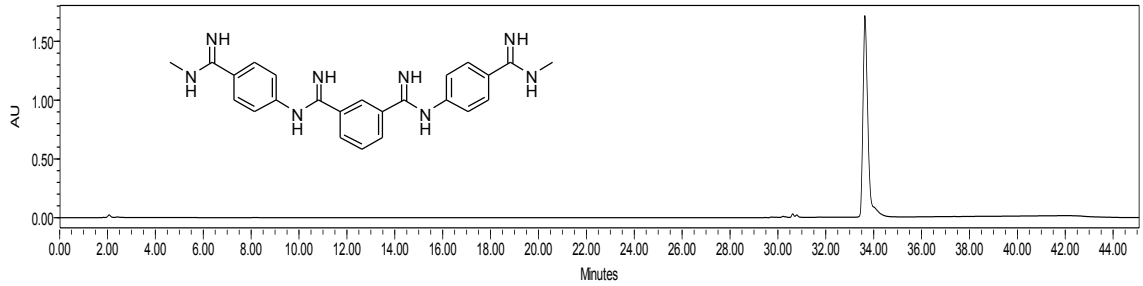

Figure S-11: Analytical HPLC trace of P8.

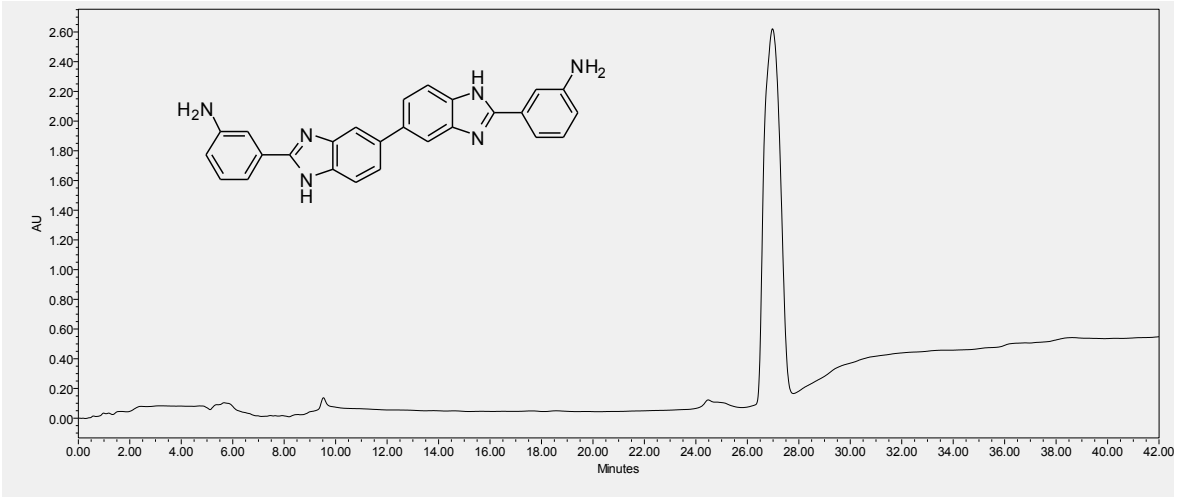

Figure S-12: Analytical HPLC trace of H1.

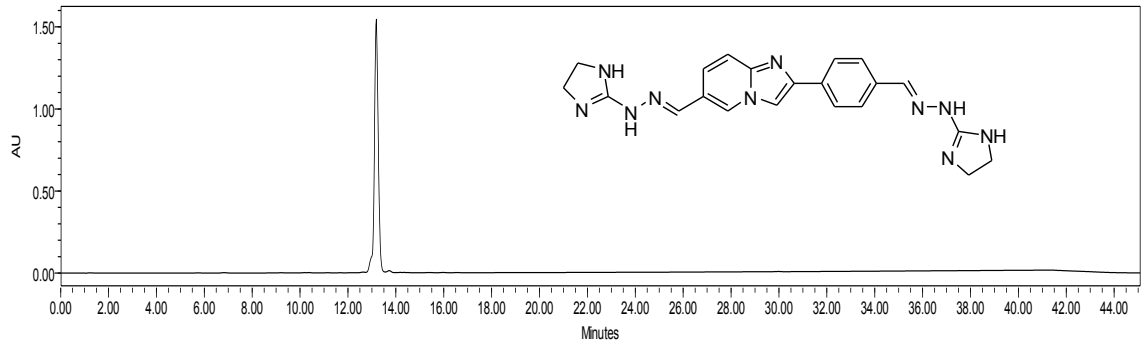

Figure S-13: Analytical HPLC trace of H2.

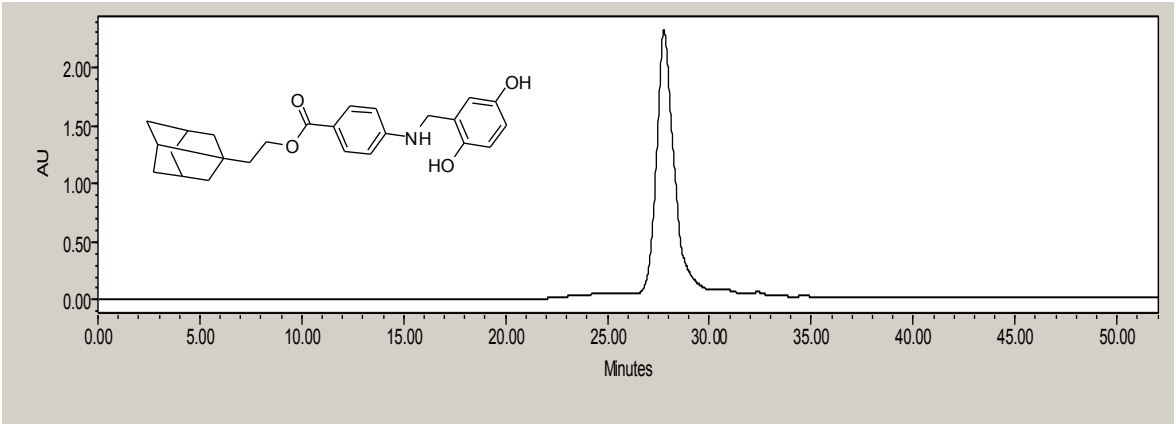

Figure S-14: Analytical HPLC trace of H3.

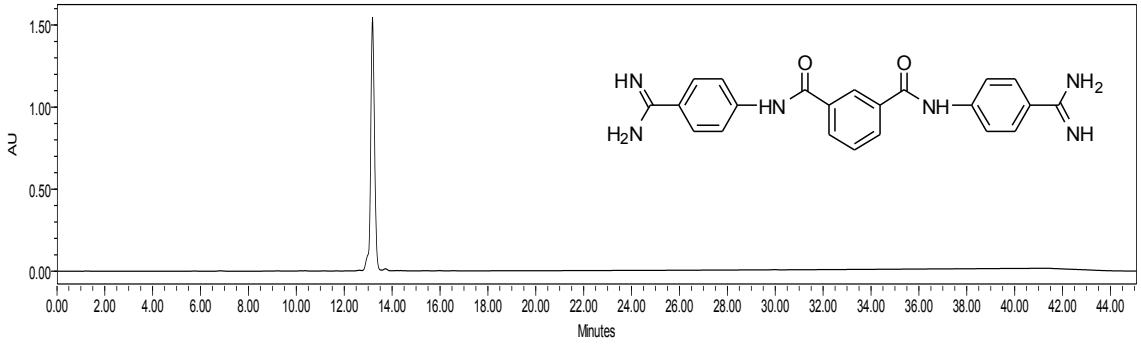

Figure S-15: Analytical HPLC trace of H4.

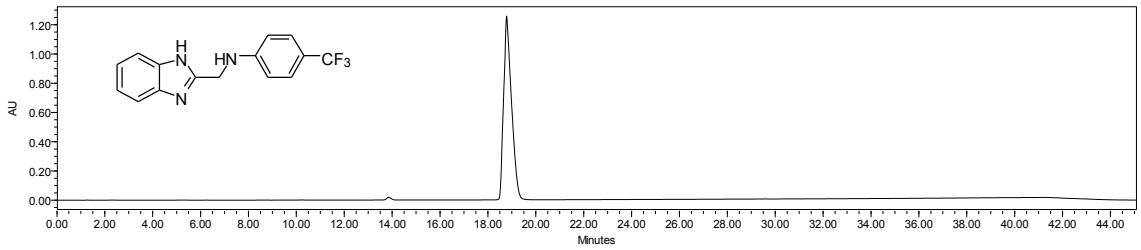

Figure S-16: Analytical HPLC trace of H5.

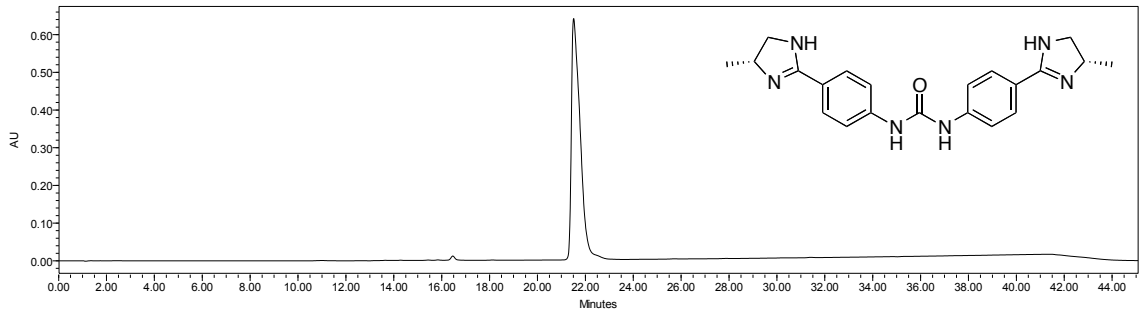

Figure S-17: Analytical HPLC trace of H6.

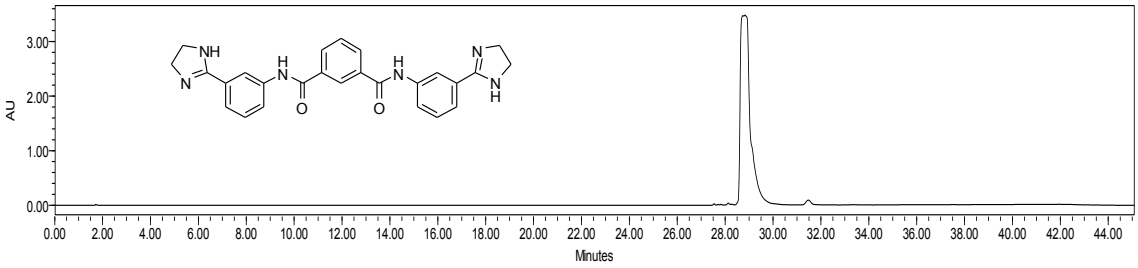

Figure S-18: Analytical HPLC trace of H7.

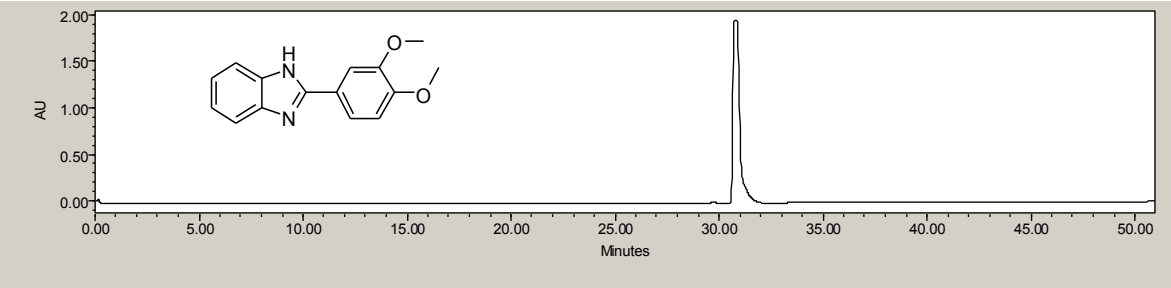

Figure S-19: Analytical HPLC trace of H8.

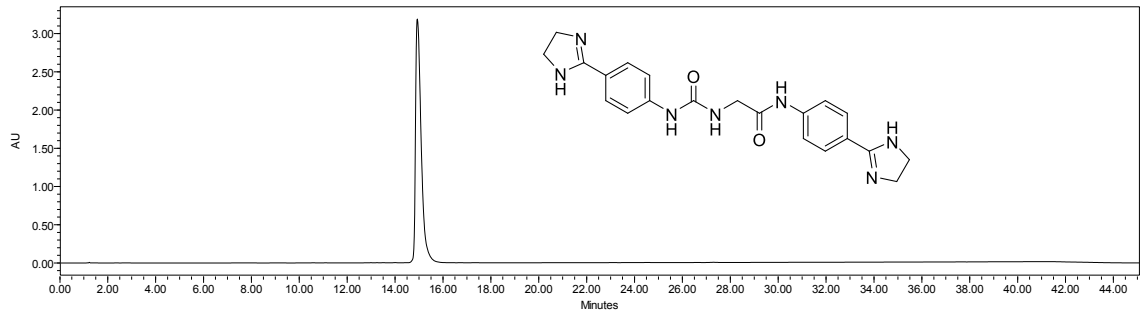

Figure S-20: Analytical HPLC trace of H9.

6. Complete List of all Compounds Screened Using a FRET-Based Assay

Table S-3: List of compounds screened for inhibition of r(CUG)$_{12}$-MBNL1 complex formation.

Compound ID (NSC Number or Catalog ID)	Manuscript ID	Source	Query Molecule	Combo Score	Percentage Inhibition at 1 mM	IC_{50} (μM)
4310	-	NCI	Hoechst	1.11	3	-
51187	H7	NCI	Hoechst	1.15	74	500
52103	-	NCI	Hoechst	1.16	66	-
54093	-	NCI	Hoechst	1.10	0	-
54696	-	NCI	Hoechst	1.10	23	-
55149	H4	NCI	Hoechst	1.12	79	200
56908	H5	NCI	Hoechst	1.04	95	300
61904	-	NCI	Hoechst	1.11	41	-
63665	-	NCI	Hoechst	1.13	51	-
63679	H6	NCI	Hoechst	1.13	89	375
78640	H9	NCI	Hoechst	1.08	93	500
106206	-	NCI	Hoechst	1.16	18	-
113089	-	NCI	Hoechst	1.12	0	-
114702	-	NCI	Hoechst	1.08	25	-
127160	-	NCI	Hoechst	1.16	15	-
134398	-	NCI	Hoechst	1.13	3	-
164156	-	NCI	Hoechst	1.07	30	-
164512	-	NCI	Hoechst	1.05	25	-
176319	-	NCI	Hoechst	1.15	0	-
211738	-	NCI	Hoechst	1.20	38	-
215651	-	NCI	Hoechst	1.12	36	-
311153	-	NCI	Hoechst	1.04	0	-
319463	-	NCI	Hoechst	1.09	6	-
347198	-	NCI	Hoechst	1.05	18	-
353884	-	NCI	Hoechst	1.16	46	-
371682	-	NCI	Hoechst	1.09	0	-
375162	H2	NCI	Hoechst	1.21	84	60
377363	-	NCI	Hoechst	1.16	0	-
403435	H8	NCI	Hoechst	1.03	83	500
600523	-	NCI	Hoechst	1.19	66	-
600815	-	NCI	Hoechst	1.10	18	-
697709	-	NCI	Hoechst	1.11	8	-
699145	-	NCI	Hoechst	1.01	71	-
719177	H3	NCI	Hoechst	1.12	96	125
000A-0377	-	ChemDiv	Hoechst	1.38	68	-
3226-1099	-	ChemDiv	Hoechst	1.56	24	-

3616-1805	-	ChemDiv	Hoechst	1.36	0	-
5057-2468	H1	ChemDiv	Hoechst	1.63	92	50
6843-3168	-	ChemDiv	Hoechst	1.56	0	-
D299-0118	-	ChemDiv	Hoechst	1.35	3	-
G796-0433	-	ChemDiv	Hoechst	1.25	30	-
G796-0435	-	ChemDiv	Hoechst	1.24	15	-
114971	-	NCI	Pentamidine	1.06	25	-
11506	-	NCI	Pentamidine	1.16	59	-
17602	-	NCI	Pentamidine	1.11	0	-
37166	-	NCI	Pentamidine	1.36	0	-
52087	-	NCI	Pentamidine	1.14	48	-
55146	P2	NCI	Pentamidine	1.47	73	50
55151	P6	NCI	Pentamidine	1.33	86	375
55153	-	NCI	Pentamidine	1.17	64	-
64897	P3	NCI	Pentamidine	1.30	83	60
66759	P8	NCI	Pentamidine	1.55	80	1000
71199	P4	NCI	Pentamidine	1.13	100	200
77879	P1	NCI	Pentamidine	1.45	80	10
77889	-	NCI	Pentamidine	1.47	30	-
80968	-	NCI	Pentamidine	1.51	48	-
105893	-	NCI	Pentamidine	1.12	0	-
169415	-	NCI	Pentamidine	1.19	68	-
179203	-	NCI	Pentamidine	1.31	43	-
190764	-	NCI	Pentamidine	1.21	48	-
210467	P7	NCI	Pentamidine	1.07	95	375
211726	P5	NCI	Pentamidine	1.36	89	250
211799	-	NCI	Pentamidine	1.23	61	-
290510	-	NCI	Pentamidine	1.13	36	-
302569	-	NCI	Pentamidine	1.37	48	-
303254	-	NCI	Pentamidine	1.14	32	-
305825	-	NCI	Pentamidine	1.81	33	-
305831	-	NCI	Pentamidine	1.26	0	-
305836	-	NCI	Pentamidine	1.26	0	-
322921	-	NCI	Pentamidine	1.84	57	-
364277	-	NCI	Pentamidine	1.34	68	-
369723	-	NCI	Pentamidine	1.43	41	-
377363	-	NCI	Pentamidine	1.54	0	-
405275	-	NCI	Pentamidine	1.08	0	-
607617	-	NCI	Pentamidine	1.49	0	-

7. Representative Autoradiograms of RT-PCR Analysis to Assess Improvement of Splicing Defects

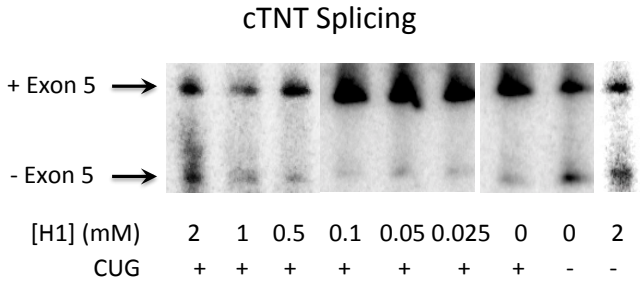

Figure S-21: H1 improves cTNT splicing defects in HeLa cells co-transfected with a plasmid encoding 960 interrupted CTG repeats and a cTNT mini-gene. Representative autoradiogram.

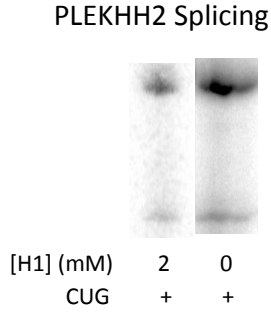

Figure S-22: H1 does not affect PLEKHH2 splicing, which is not controlled by MBNL1.

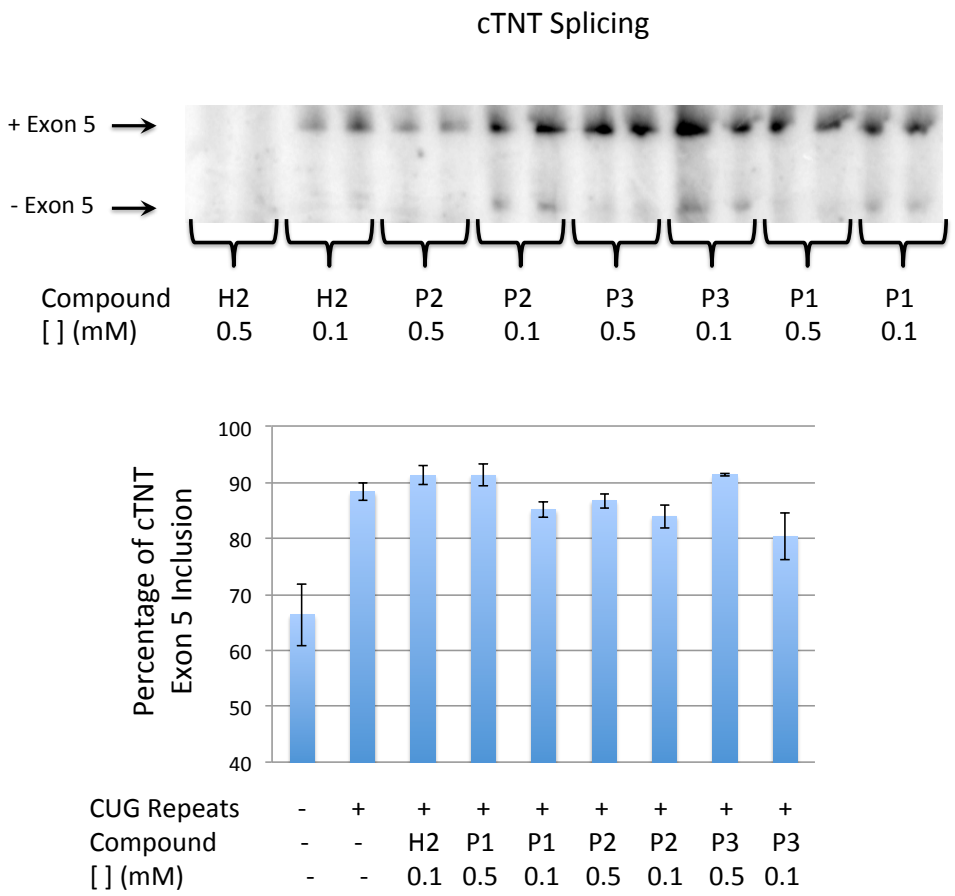

Figure S-23: H2, P1, P2, and P3 have little effect on cTNT splicing defects in HeLa cells co-transfected with a plasmid containing 960 interrupted CTG repeats and a cTNT mini-gene. The cTNT mini-gene splicing products could not be RT-PCR amplified when cells were treated with 0.5 mM H2, indicating that the compound could be toxic. P1, P2, and P3 do not improve cTNT splicing when the cells are treated with 0.5 mM compound.

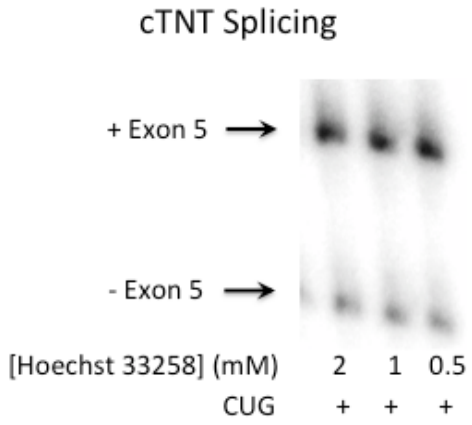

Figure S-24: Hoechst 33258 does not improve cTNT splicing defects in HeLa cells co-transfected with a plasmid containing 960 interrupted CTG repeats and a cTNT mini-gene. Hoechst 33258 does not improve cTNT splicing when the cells are treated with up to 2 mM compound.

8. Representative Binding Curve for the Binding of H1 to an RNA Containing the DM1 Motif

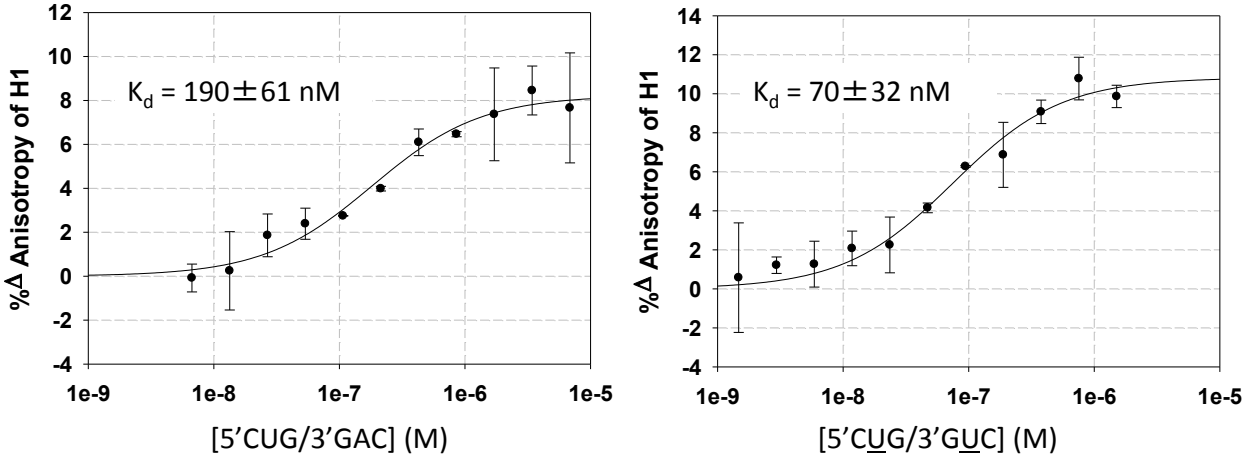

Figure S-25: Representative binding curves used to determine the affinity of H1 for a fully paired RNA (left) and an RNA with a single 5'CUG/3'GUC (DM1) (right). The affinities were determined by monitoring the change in anisotropy of H1 as a function of RNA concentration. The resulting curves were fit to: $y = (B_{max}*x) / (K_d + x)$, where y is the observed anisotropy intensity, B_{max} is the maximum anisotropy observed, x is the concentration of RNA and K_d is the dissociation constant.

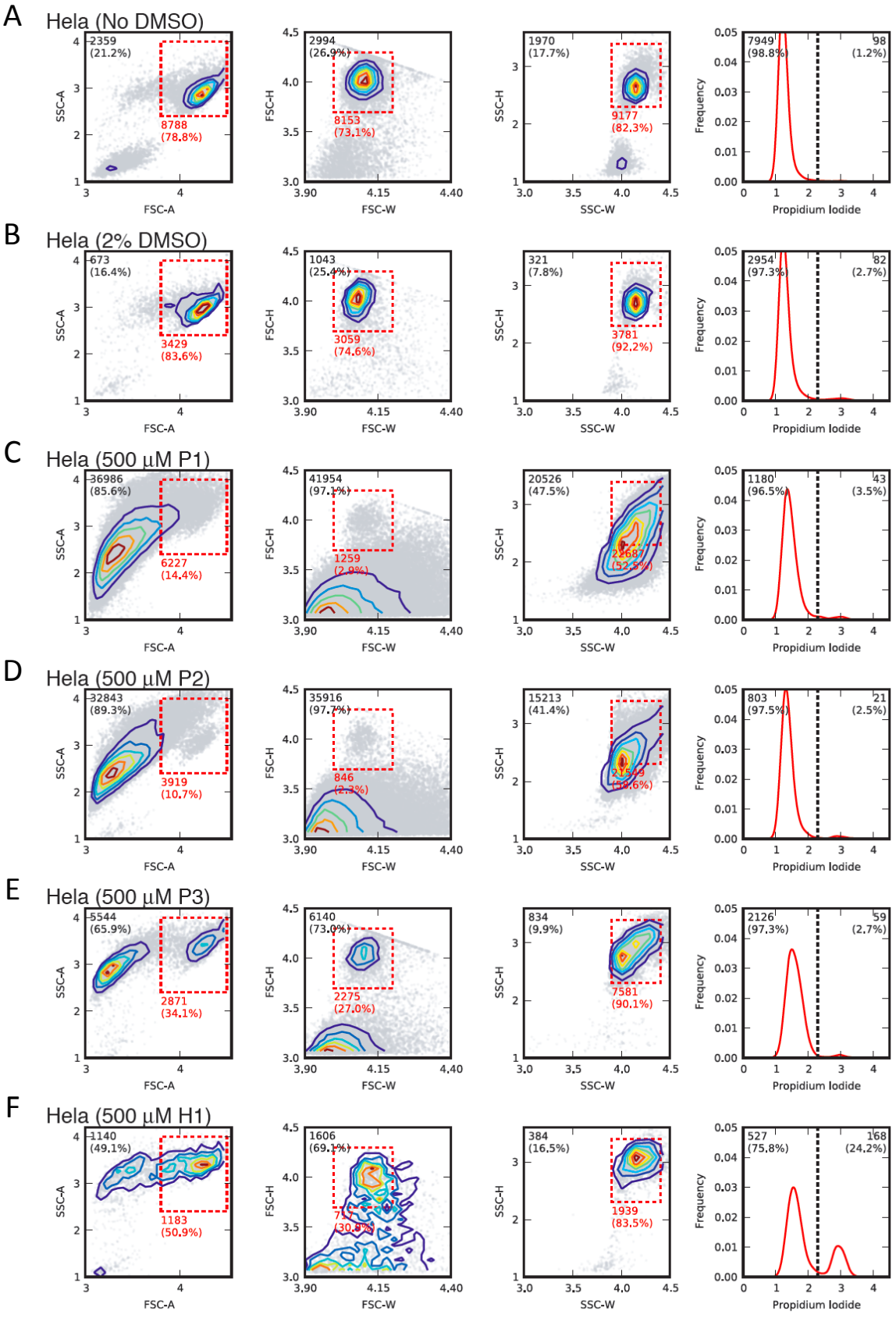
A
Hela (No DMSO)
2359
(21.2%)
8788
(78.8%)
2994
(26.9%)
8153
(73.1%)
1970
(17.7%)
9177
(82.3%)
7949
(98.8%)
98
(1.2%)
B
Hela (2% DMSO)
673
(16.4%)
3429
(83.6%)
1043
(25.4%)
3059
(74.6%)
321
(7.8%)
3781
(92.2%)
2954
(97.3%)
82
(2.7%)
C
Hela (500 µM P1)
36986
(85.6%)
6227
(14.4%)
41954
(97.1%)
1259
(2.9%)
20526
(47.5%)
22687
(52.5%)
1180
(96.5%)
43
(3.5%)
D
Hela (500 µM P2)
32843
(89.3%)
3919
(10.7%)
35916
(97.7%)
846
(2.3%)
15213
(41.4%)
21549
(58.6%)
803
(97.5%)
21
(2.5%)
E
Hela (500 µM P3)
5544
(65.9%)
2871
(34.1%)
6140
(73.0%)
2275
(27.0%)
834
(9.9%)
7581
(90.1%)
2126
(97.3%)
59
(2.7%)
F
Hela (500 µM H1)
1140
(49.1%)
1183
(50.9%)
1606
(69.1%)
384
(16.5%)
1939
(83.5%)
527
(75.8%)
168
(24.2%)
FSC-A
FSC-H
FSC-W
SSC-A
SSC-H
SSC-W
Frequency
Propidium Iodide

Figure S-26: Flow cytometry analysis of cells treated with compounds. HeLa cells were treated with 500 μM P1, P2, P3, or H1 (in media with 2% DMSO) for 16 h and analyzed by flow cytometry, using standard forward and side scatter metrics, and propidium iodide (PI) staining. Cells were compared to those treated with 2% DMSO for 16 h (Panel B) and those grown in media alone (Panel A). Four plots are shown for each treatment condition (from left to right): forward scatter area (FSC-A) vs. side scatter area (SSC-A), forward scatter width (FSC-W) vs. forward scatter height (FSC-H), side scatter width (SSC-W) vs. side scatter height (SSC-H), and a histogram of PI staining for cells selected in the gates outlined by red dashed lines.

The number of particles, or events, observed by the flow cytometer is displayed, where events lying within the gates are shown in red text and those outside are shown in black text. The gates illustrated are those typically used to select healthy cells. PI stains cells that are still grossly intact but permeabilized; treatment of cells with DMSO results in a slight increase in the percentage of cells stained with PI.

Notably, treatment with P1 (Panel C) and P2 (Panel D) yield a large number of observed events with low forward scatter area and height values, indicating that most observed events represent cell debris. Treatment of cells with P3 (Panel E) also leads to loss of cell integrity but to a lesser extent. Following H1 treatment (Panel F), over half of cells still remain within each gate, indicating that cell integrity is largely preserved.

PI staining provides quantitation of the extent to which intact cells are permeable. As mentioned previously, treatment of the cells with P1, P2, and P3 leads to loss of cell integrity as evidenced by their low forward scatter area and height values. This cellular debris does not stain with propidium iodide, since propidium iodide stains DNA in intact cells, as reflected in the PI histograms. In contrast, most of the cells treated with H1 are largely intact; some are permeabilized and therefore contain DNA stained with PI. In summary, H1 is by far the least cytotoxic compound as compared to P1, P2, and P3.

REFERENCES

1. Wilson, F. X., Johnson, P. D., Vickers, R., Storer, R., Wynne, G. M., Roach, A. G., De, M. O., Dorgan, C. R., and Davis, P. J. (2010) Preparation of bibenzo[d]imidazoles and other biheteroaryl compounds as antibacterial agents, (WO2010063996 A2).